

Overview of the MSTI 2 On-Orbit Alignment

Christopher A. Rygaard
Fred W. Smith
M. Michael Briggs

Integrated Systems, Inc.
Santa Clara, CA

Abstract

The Miniature Sensor Technology Integration (MSTI) 2 spacecraft is a small 3-axis stabilized spacecraft designed to track mid-range missiles and estimate their state vectors. In order to accurately estimate the target state vector, the MSTI 2 spacecraft must have high accuracy knowledge of its own attitude. Errors in its attitude knowledge arise primarily from the errors in its Attitude Control System (ACS) sensors. The ACS sensors on the spacecraft include a scanning Earth Sensor (ES), a Sun Sensor (SS), and two 2-axis gyros.

The On-Orbit Alignment (OOA) generated an error map of the ES, and estimated the biases of the SS and the misalignment of the gyros. This paper discusses some of the error sources, and the techniques used to reduce the effects of these errors, including estimating errors so that they could be analytically eliminated, and mission design to avoid these errors.

The payload carried by the MSTI 2 spacecraft is a high fidelity camera, which was aimed at the target using gimballed mirrors. By aiming it at a celestial target, the payload was used as a high-accuracy single-axis attitude reference. This attitude reference was compared to the attitude reference of the ACS sensors, and the errors were attributed to the ACS sensors.

Introduction

The MSTI 2 spacecraft (see Figure 1) was designed to track theater ballistic missiles and estimate their state vector. This requires that the attitude knowledge of the spacecraft be on the order of 100 microradians.

The payload is a high accuracy camera with a gimballed mirror. The payload can lock onto a target and track it independently of the MSTI 2 bus. By using the payload to track Venus, it provided a high-fidelity single-axis attitude reference. The ACS sensor data was compared to this attitude reference in order to estimate their respective errors.

This paper discusses some of the error sources, and the techniques used to reduce the effects of these errors, including the estimation techniques to determine some of these errors, and the mission design techniques to avoid other of these errors.

The ACS sensors include two 2-axis gyros, an earth sensor, and a sun sensor. Each of these sensors was calibrated independently, and this paper presents the approach used in each of these calibrations.

Error sources

The gyros underwent extensive ground testing, and were very well characterized prior to launch. The primary error source for the gyros is due to geometric misalignment in their mounting on the spacecraft.

The ground testing of the sun sensor indicated errors on the order of 0.2° , while ground testing of the earth sensor indicated errors on the order of 0.1° . It was unclear if these errors were within the sensor itself, or if they were due to inaccuracies in the test apparatus. In addition, the ground testing included no statistical characterization. Also, the time-tagging of the SS data and ES included a uniform-distribution error 0.2 seconds wide. The SS and ES also had errors due to geometric misalignment their mounting on the spacecraft.

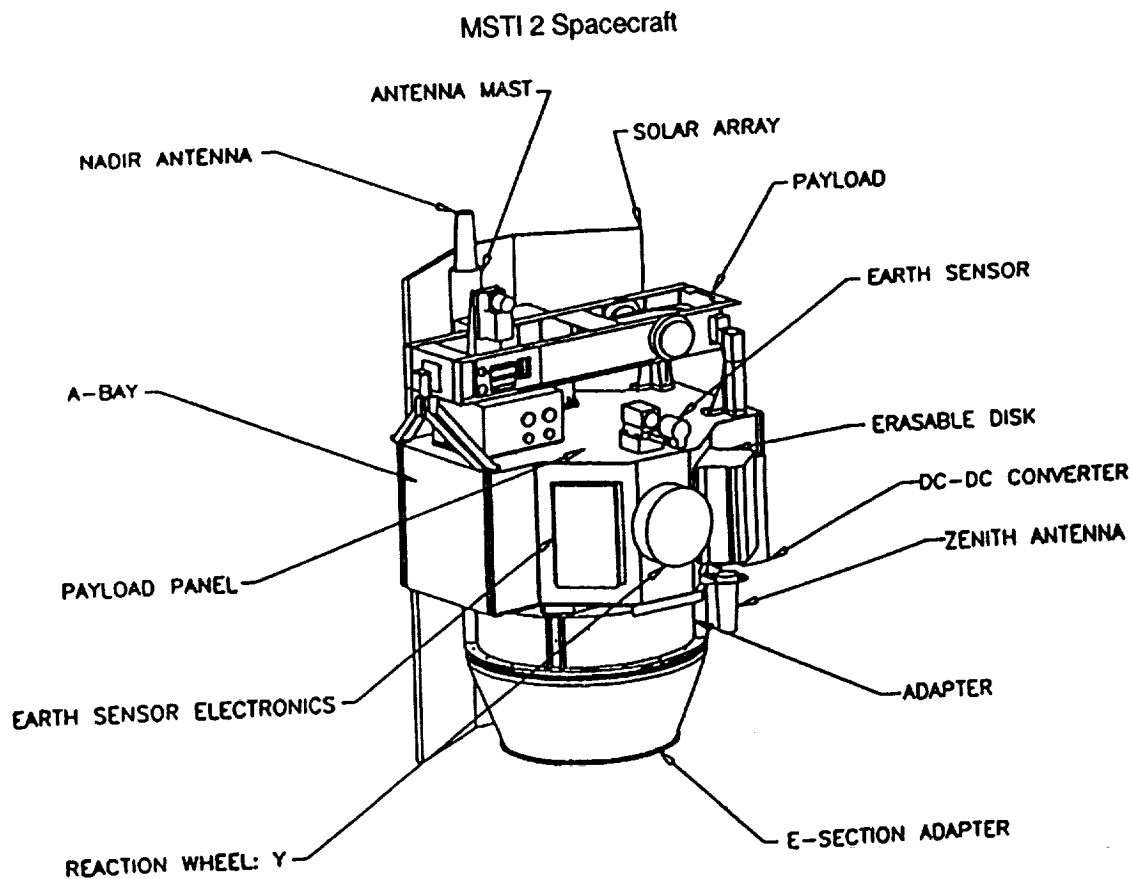


Figure 1

The earth sensor had two other error sources. First, the relatively slow scan rate of the ES caused an error source in its attitude information. If the spacecraft is slewing, the spacecraft will slew a certain amount during the time between sensing the leading edge of the earth signal and sensing the trailing edge of the earth signal. The amount of this slew would introduce errors in the attitude knowledge. Second, the flight software analyzed the ES data under a spherical earth shape approximation. This can introduce errors as large as 1° . The OOA and the mission design had to account for this error source by utilizing an oblate earth shape approximation.

The goal of the MSTI 2 bus is to accurately point the payload. Therefore it was decided that the ACS sensors would be calibrated relative to the p_1 , p_2 , and p_3 unit vectors which define the payload reference frame, and not relative to the S/C frame. This eliminated any errors due to uncertainties in the precise location of the S/C reference frame. In fact, the attitude of the S/C reference frame is irrelevant during a target encounter; only the attitude of the payload is of interest. The S/C reference frame is completely fictitious; it is a purely mathematical construct to facilitate analysis, design, and construction.

Mission Design to Avoid Errors

The problem of the slow ES scan rate is eliminated if the spacecraft is not slewing, because there will be no change in attitude between the times of the leading edge and the trailing edge of the earth signal. Also, the time-tagging problem of the ES and the SS is eliminated if the spacecraft is not slewing, because the signals they generate are constant. Therefore it was decided that immediately prior to a target encounter, the spacecraft would hold its attitude fixed in inertial space long enough to obtain a high accuracy attitude reference, and then proceed with the target encounter using only gyro propagation. This maneuver was called the "Gyro Nulling Attitude" (GNA). The GNA effectively eliminated the error sources due to time tagging and slow ES scan rate. This in turn eliminated the need to analytically remove the errors due to these sources.

The primary purpose of the GNA was to hold the spacecraft fixed in inertial space in some attitude. This maneuver would be effective in any orientation. Therefore, it was decided to select the GNA orientation to reduce the OOA effort. Ideally, it would be necessary to calibrate only one point in the SS FOV, and one single ES orientation, and then select the GNA to place the sun and earth at these points. With this technique, the error estimation effort of the

OOA would be greatly reduced. However, the Sun-S/C-Earth angle changes during the spacecraft's orbit around the earth, and it changes during the earth's orbit around the sun. Therefore, these sensors had to be calibrated to accommodate a range of Sun-S/C-Earth angles. Nonetheless, this approach reduced the error estimation effort significantly.

Celestial Attitude Reference

The only celestial bodies which are bright enough to be seen by the MSTI 2 payload are the sun, the moon, and Venus. The sun could not be used because it would quickly damage the focal plane of the payload.

The moon is bright enough to be tracked by the payload, but it has a significant angular extent as seen from orbit. In addition, its image on the MSTI 2 payload focal plane will have some unknown shape due to the cooling of the moon as it changes phases, and it is unclear exactly how the tracker would compute the centroid of this shape. The only feasible technique to use the moon as an attitude reference would have required that the outer arc of the crescent of the moon be estimated, so that its center could be used as an accurate attitude reference. This implies an extensive development effort with high risk.

Therefore, it was decided that Venus would be used as the celestial attitude reference. This presented its own set of problems. The off-axis sensitivity of the MSTI 2 payload is such that if it is pointed within 20° of the sun, any image it has would be washed out. Figure 2 shows the separation between Venus and the sun during the period of interest. Prior to April 9, 1994, Venus is within 20° of the sun. This was only a few days prior to the MSTI 2 OOA maneuvers.

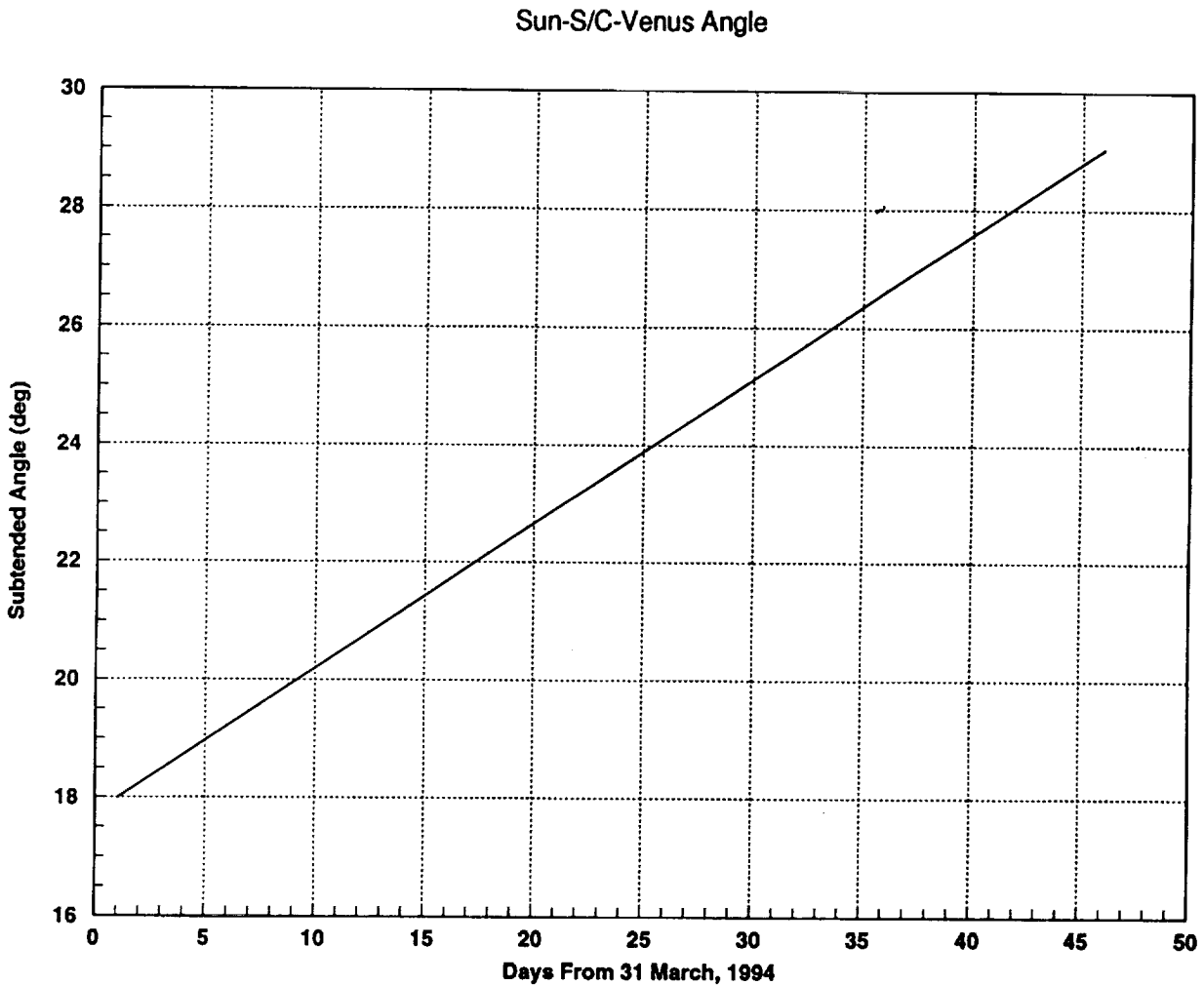


Figure 2

In addition, this small subtended angle between the sun and Venus presented problems arising from the geometry of the MSTI 2 spacecraft, as will be described in the discussion on SS calibration.

Sun Sensor Calibration

The SS has a "square" Field Of View (FOV), nominally centered along the S/C Y axis. The sun sensor would report the position of the sun by transmitting two signed angles representing the location of the sun in the FOV. These are (1) SS Z, the angle between the projection of a unit vector pointing toward the sun onto the S/C X-Y plane, and the S/C X axis, and (2) SS X, the angle between the projection of a unit vector pointing toward the sun onto the S/C Z-Y plane and the S/C Z axis.

Due to geometry constraints, it was decided that only one point in the SS FOV would be calibrated, as described below. A complete calibration at this single point could be characterized by a simple bias on each of the two outputs. Because it is a single point, all of the non-temporal error sources could be corrected by these simple biases.

The approach utilized to estimate these biases was purely geometric. With this approach, in order to measure the errors with a single experiment, the full 3-axis attitude of the payload reference frame would have to be known. However, the only high-accuracy attitude reference available was Venus, and this was only a single-axis attitude reference. Therefore, multiple experiments were required in order to make the biases observable. This purely geometric approach ignores the information provided by the gyros, but it also keeps the gyro alignment estimation and the SS calibration independent of each other.

The approach utilized is illustrated in Figures 3 and 4. These figures are for descriptive purposes only, and are not drawn to scale. Figure 3 illustrates one procedure, and Figure 4 illustrates another procedure. These two procedures alone are enough to algebraically determine the biases. Multiple executions of these two procedures provided statistical data and required a least-squares estimator.

In Figure 3 (Procedure #1), the sun is located in the SS FOV at the calibration point. Also Venus is in the FOR of the payload at one location, which provides only one axis of attitude information. Using astronomical databases, β_1 , the subtended angle between the sun and Venus, is known very accurately. Therefore it is known that the sun must lie somewhere along the arc shown in Figure 3. The exact location of the sun along this arc is unknown because the Venus vector provides only one axis of attitude information. This procedure, by itself, provides only partial error information. In particular, it provides only ϵ_{p1} , the component of the error normal to the arc in Figure 3. In Figure 4 (Procedure #2), the S/C is oriented so that the sun is still at the calibration point, but Venus is located at a different point in the payload FOR. In effect, the S/C has slewed about the S/C-sun line from Procedure #1 to Procedure #2. Again, this procedure, by itself, only provides partial error information, ϵ_{p2} . Combining the results from Procedure #1 and #2 will provide full error information, because the errors measured in the two experiments are in different directions.

The procedures depicted in Figures 3 and 4 were each executed several times in order to obtain some statistical characterization of the results.

In addition to estimating the SS errors, the combination of Procedures #1 and #2 will also provide enough information to determine the slew angle about the S/C-Venus line for each experiment.

In the least-squares estimator, the vector of estimated parameters was

$$\mathbf{x} = \begin{bmatrix} \zeta_1 \\ \zeta_2 \\ \dots \\ \zeta_n \\ \epsilon_x \\ \epsilon_z \end{bmatrix}$$

Where ζ_i is the slew angle about the S/C-Venus line for procedure #i ($i=1, \dots, n$), ϵ_x is the bias in the SS X measurement at the calibration point and ϵ_z is the SS Z measurement bias at the calibration point. It was necessary to estimate the individual slew angles because it indirectly provided a 3-axis attitude determination for each procedure, and this is what is required for measuring the SS errors.

Sun Sensor Estimation Procedure #1

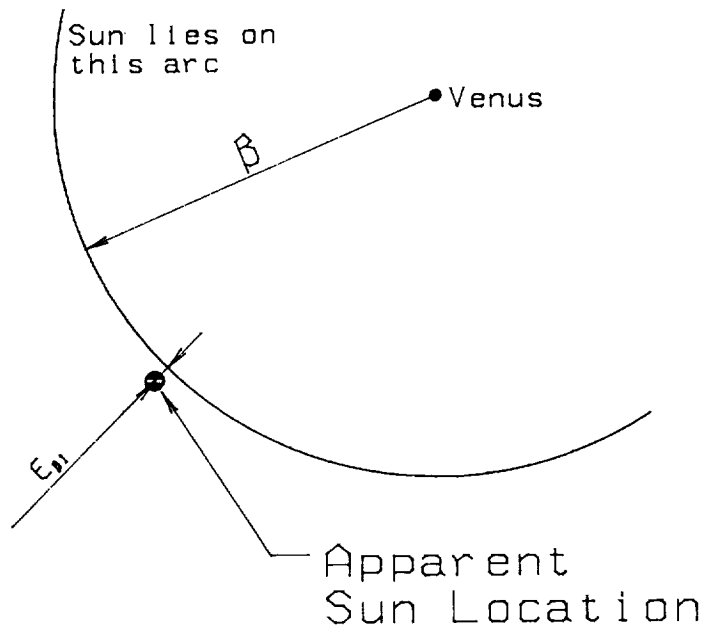


Figure 3

Sun Sensor Estimation Procedure #2

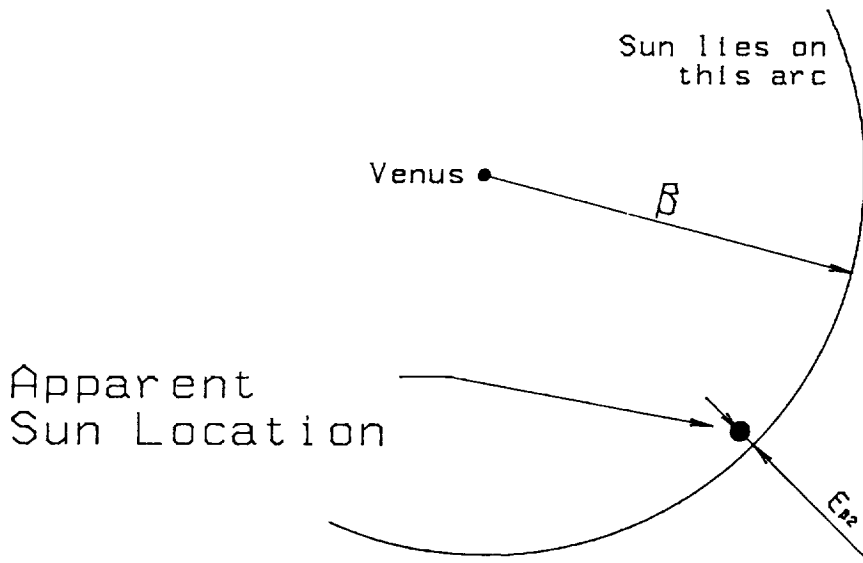


Figure 4

The measurement vector used for the SS estimation was:

$$m = \begin{bmatrix} SSX_1 \\ SSZ_1 \\ SSX_2 \\ SSZ_2 \\ \vdots \\ SSX_n \\ SSZ_n \end{bmatrix}$$

Where SSX_i and SSZ_i are the two outputs of the SS for procedure #i ($i=1, \dots, n$).

Because only data from the SS and the payload were used, the calibration was necessarily relative to the frame defined by the payload, and not relative to the S/C frame.

Figure 5 shows the geometry of the payload FOR relative to the SS FOV. In this polar plot, the radial dimension represents the angle from the payload Z axis, and the angular dimension represents the azimuth from the payload X axis. The solid line represents the limits of the payload FOR, and the dashed line represents the limits of the SS FOV. Not all of the SS FOV is shown in Figure 5. The Field Of Regard of the MSTI 2 payload was limited by the amount of travel allowed in the gimbals.

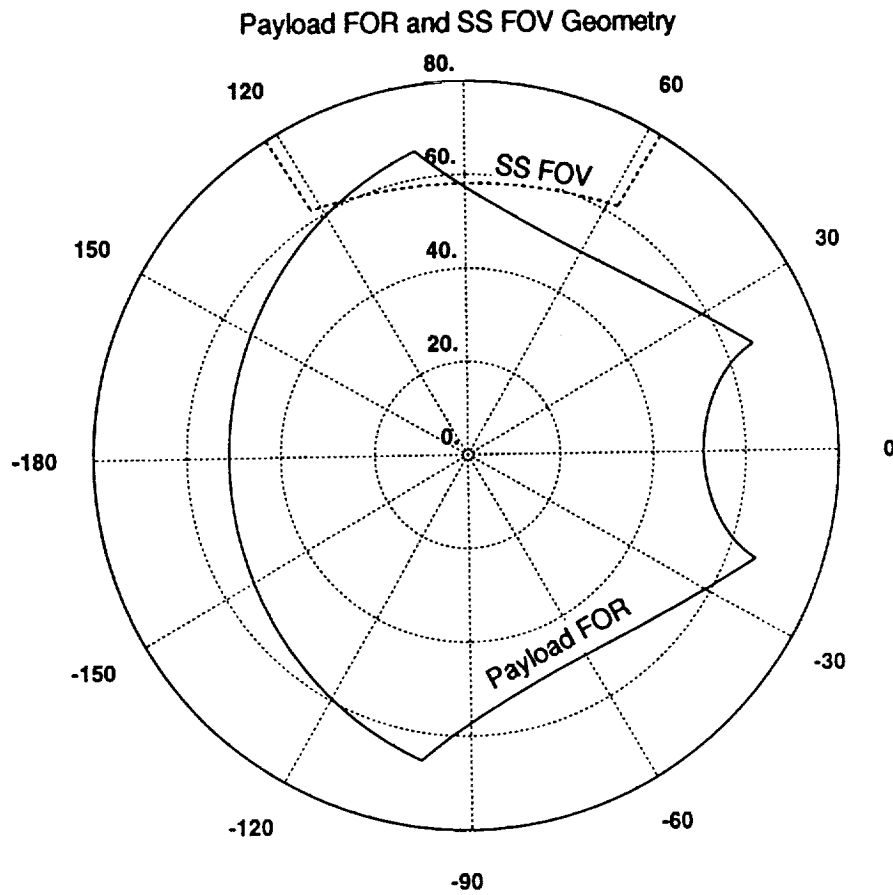


Figure 5

When the payload is pointed near the edge of its FOR, its image will be partially obscured by the S/C structure, resulting in a dimmer image. Therefore, it is desirable to point the S/C so that Venus is as far away from the edge of the FOR of the payload as possible. This places a limitation on the geometries which will simultaneously place the sun in the SS FOV and Venus in the payload FOR.

During the time of the OOA maneuvers, the Venus was 20° to 30° away from the sun, as indicated in Figure 2. This, coupled with Figure 5, indicates additional limitations on geometries which will simultaneously place Venus in the payload FOR and the sun in the SS FOV.

These limitations were the driving factors in the decision to calibrate the SS at only one point. The calibration point, and the geometries of the SS calibration experiments, are illustrated in Figure 6. By selecting the calibration point at $SSX = 30^\circ$ and $SSZ = 10^\circ$, Venus was kept as far away from the edges of the payload FOR, while still allowing a 90° slew about the S/C-sun line between the two procedures. The small circle is the chosen location of the SS calibration point, and the two "x"s represent the location of Venus for the two SS Calibration maneuvers.

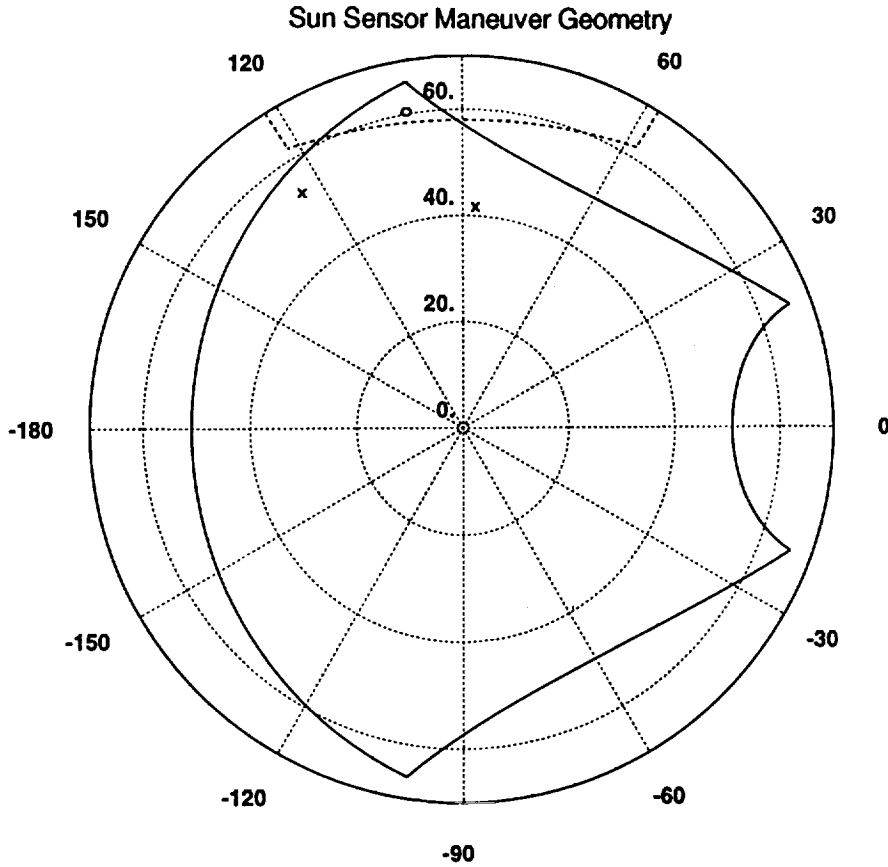


Figure 6

For maximum observability, the slew angle about the S/C-sun line between the two experiments should be 90° . The two Venus locations indicated in Figure 5 satisfy this requirement.

Earth Sensor Calibration

The ES is a scanning horizon sensor. It has a 2° conical field of view which sweeps out a cone with a 60° half-cone angle every 0.2 seconds. The axis of the ES scan cone is nominally along the S/C -Y axis. The ES measures the size and location of the "earth chord", which is that portion of the scan cone which intersects the earth. The outputs of the ES consist of Φ , the scan angle from a zero-reference scan angle to the center of the earth chord, and Ω , the width of the earth chord.

The basic technique to calibrate the ES is similar to the SS calibration. The primary differences are:

- (1) The geometry of a scanning horizon sensor is different from the geometry of the SS,
- (2) The ES had to be calibrated along a locus of points to accommodate a range of earth-S/C-sun angles,
- (3) No analytic horizon sensor model incorporating an oblate earth shape model was available.

Because of the complicated geometry of a scanning horizon sensor, the location of the earth in the S/C frame was deduced only indirectly. Because an oblate earth shape model was required, there were no analytic expressions relating the location of the earth to the ES sensor readings. An iterative search was employed, using the spherical

earth shape approximation as a first guess.

Because the Sun-S/C-earth angle changes during the orbit and during the year, and because only one point of the SS FOV was calibrated, it was necessary to calibrate a locus of ES output pairs to cover the range of possible angles. Each "point" in the locus corresponded to one location of the earth relative to the payload frame.

The multiple procedure technique described above for the SS calibration was modified for the ES calibration. There were two sets of procedures, instead of two discrete procedures. For each procedure in the first set, the S/C was oriented so that the earth was at various points along the calibration locus, and all of these procedures used approximately the same slew angle about the S/C-earth line. For the second set of procedures, the earth was again located at various points along the calibration line, but the slew angle about the S/C-earth line was approximately 90° from the slew angle used for the first set.

Because the ground testing included no statistical characterization, an assumed function with unknown parameters was used to model the ES errors. The Φ and Ω errors were each assumed to vary as a function of the distance along the locus of points. Because an assumed form of the error model was used, it was unnecessary to calibrate individual points with pairs of parameters, as was done with the SS calibration. Instead, the error function parameters were estimated collectively. It was only necessary that each individual procedure placed the earth at some location along the locus. It was not necessary for each procedure in the second set of procedures to place the earth at the same location along the locus as an procedure in the first set.

In the least-squares estimator, the vector of estimated parameters was:

$$\mathbf{x} = \begin{bmatrix} \alpha_1 \\ \alpha_2 \\ \vdots \\ \alpha_{n-1} \\ \alpha_n \\ c_{\phi 0} \\ c_{\phi 1} \\ c_{\phi 2} \\ c_{\Omega 0} \\ c_{\Omega 1} \\ c_{\Omega 2} \end{bmatrix}$$

Where α_i is the slew angle about the S/C-Venus line for experiment #i ($i=1, \dots, n$), and $c_{\phi 0}$, $c_{\phi 1}$, $c_{\phi 2}$, $c_{\Omega 0}$, $c_{\Omega 1}$, and $c_{\Omega 2}$ are the unknown parameters of the ES error model. It was necessary to estimate the individual slew angles because it indirectly provided a 3-axis attitude determination for each experiment, and this is what is required for measuring the ES errors.

The measurement vector used was:

$$\mathbf{m} = \begin{bmatrix} \Phi_1 \\ \Omega_1 \\ \Phi_2 \\ \Omega_2 \\ \vdots \\ \vdots \\ \Phi_n \\ \Omega_n \end{bmatrix}$$

Where Φ_i and Ω_i are the two outputs of the ES for experiment #i ($i=1, \dots, n$).

The least-squares estimator requires derivatives of the measurement vector elements with respect to the state vector elements. Because no analytic function relating Φ and Ω to the estimated parameters was available, there was no analytic expression for the related derivatives. However, the spherical earth shape model is very nearly equal to the oblate earth shape model, so the derivatives based on the spherical earth shape model were used, while the measurement model used the oblate earth shape model.

Because only data from the ES and the payload were used, the calibration was necessarily relative to the frame defined by the payload, and not relative to the S/C frame.

Gyro Misalignment Estimation

The ground testing of the MSTI 2 gyros was very extensive, and provided very good characterization of the gyros. The gyro models, and their parameters, were determined with very good accuracy, and it was felt that no further of the gyros themselves was needed. The only significant error source in the gyros was their geometric misalignment relative to the MSTI 2 S/C.

The sensitive axes of the one of the X-Y gyro are nominally aligned with the payload frame X- and Y-axes, and the sensitive axes of the X-Z gyro are nominally aligned with the payload frame X- and Z-axes. The X-axis rate information, for both attitude control and telemetry, comes from only one gyro at any given time, as selected by ground commands. The nominal mission called for using both channels of the X-Y gyro, and only the Z-axis information of the X-Z gyro. Therefore, it was necessary to estimate all three misalignment angles for the X-Y gyro, and only two misalignment angles for the X-Z gyro.

In order to make the gyro misalignments observable, three simple Euler-axis slews were executed by the S/C. While performing these slews, the payload was tracking Venus in order to make the estimated parameters observable. Ideally, for maximum observability, the three slew axes should be mutually orthogonal. However, the limited extent of the payload FOR constrained the slew axes to be non-orthogonal. The geometry of the three slews is illustrated in Figure 7. The orientation of the angular velocity vector for each slew is indicated by the small "o"s, and the dashed circles indicate the path followed by Venus through the payload FOR.

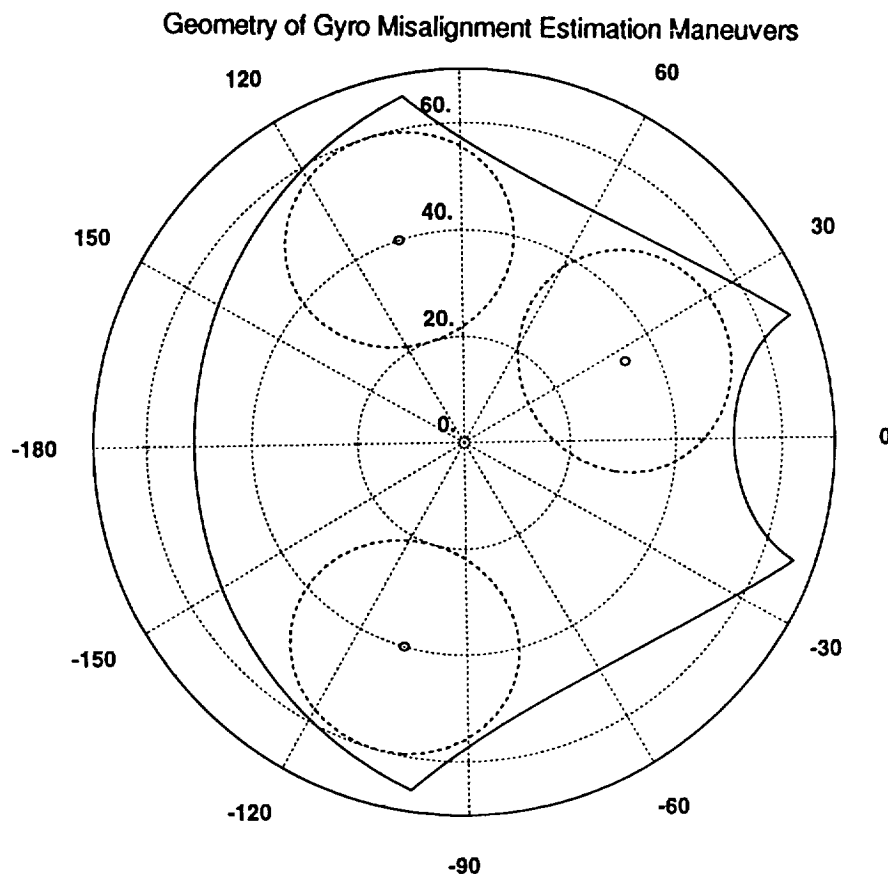


Figure 7

For this estimation, it was assumed that the two axes of each gyro are perfectly perpendicular. It was also assumed that the misalignment of each gyro was independent of the misalignment of the other gyro.

When the S/C was commanded to perform the three slew maneuvers, it complied by using the misaligned gyros. Therefore, it was necessary to also estimate the parameters of the Euler-axis slew as well as the gyro misalignments. The estimated parameters were:

- (1) The orientation and magnitude of each slew axis in the payload frame coordinates,
- (2) The orientation of each slew axis in inertial space,

- (3) The initial slew angle of each slew maneuver,
- (4) The X, Y, and Z angular misalignments of the X-Y gyro relative to the payload frame, and
- (5) The X and Y angular misalignments of the X-Z gyro relative to the payload frame.

It was necessary to express the equations describing the slew maneuvers in terms of the orientation of the slew axes in inertial space, in order to force the resulting slew parameters to apply to an Euler-axis slew fixed in inertial space. It was necessary to estimate these orientations because they were not directly measurable.

In the least-squares estimator, the vector of estimated parameters was:

$$x = \begin{bmatrix} \theta_{z01} \\ \omega_{11} \\ \omega_{21} \\ \omega_{31} \\ RA_{\alpha 1} \\ Decl_{\alpha 1} \\ \theta_{z02} \\ \omega_{12} \\ \omega_{22} \\ \omega_{32} \\ RA_{\alpha 2} \\ Decl_{\alpha 2} \\ \theta_{z03} \\ \omega_{13} \\ \omega_{23} \\ \omega_{33} \\ RA_{\alpha 3} \\ Decl_{\alpha 3} \\ \gamma_{11} \\ \gamma_{12} \\ \gamma_{13} \\ \gamma_{21} \\ \gamma_{22} \end{bmatrix}$$

Where θ_{z0i} is the initial slew angle of the S/C at the beginning of slew maneuver #i (i=1,2,3), ω_i is the component of the angular velocity vector along the p_i axis for slew maneuver #i (i=1,2,3; j=1,2,3), $RA_{\alpha i}$ is the right ascension of the angular velocity vector for slew maneuver #i (i=1,2,3), $Decl_{\alpha i}$ is the declination of the angular velocity vector for slew maneuver #i (i=1,2,3), γ_i are the three misalignment angles of the X-Y gyro (i=1,2,3), and γ_2 are two of the three misalignment angles of the the X-Z gyro (i=1,2).

The X axis data from the X-Z gyro was not available, so the third misalignment angle of the X-Z gyro, γ_{23} , is neither required nor observable.

The measurement vector used was:

$$m = \begin{bmatrix} v_{p11} \\ v_{p21} \\ v_{p31} \\ \hat{\omega}_{11} \\ \hat{\omega}_{21} \\ \hat{\omega}_{31} \\ v_{p12} \\ v_{p22} \\ v_{p32} \\ \hat{\omega}_{12} \\ \hat{\omega}_{22} \\ \hat{\omega}_{32} \\ \vdots \\ v_{p1n} \\ v_{p2n} \\ v_{p3n} \\ \hat{\omega}_{1n} \\ \hat{\omega}_{2n} \\ \hat{\omega}_{3n} \end{bmatrix}$$

Where v_{pi} is the component of the Venus unit vector along the p_i direction at time t_i ($i=1,2,3; j=1,\dots,n$), $\hat{\omega}_{1i}$ is the angular velocity measured by the X axis of the X-Y gyro at time t_i ($i=1,\dots,n$), $\hat{\omega}_{2i}$ is the angular velocity measured by the Y axis of the X-Y gyro at time t_i ($i=1,\dots,n$), and $\hat{\omega}_{3i}$ is the angular velocity measured by the Z axis of the X-Z gyro at time t_i ($i=1,\dots,n$).

Conclusion

Most of the error sources in the attitude knowledge of the MSTI 2 spacecraft were removed analytically by using the payload as a high fidelity attitude reference, and using this information to deduce the errors in the ACS sensors. This determined the errors relative to the payload, and eliminated the need to align the sensors relative to the spacecraft. Those errors which could not be eliminated analytically were avoided by careful mission design.

